



Thermal Spikes from Stopped Muons and Density Effects in
Muon-Catalyzed Fusion.

M. Jändel

CERN - Geneva

Abstract

Local hot regions caused by energy deposition from stopped and captured muons can significantly influence the cycle rate of muon catalyzed fusion. Muonic deuterium-tritium molecules are formed at a high effective temperature that increases roughly linearly with density. Optimum molecular formation rates can hence be achieved at cryogenic temperatures and high densities. The observed nonlinear density dependence of molecular formation rates is understood within this framework.

Ref.CERN-TH.4832/87

August 1987

The interest for muon-catalyzed fusion has been revived because of recent progress in increasing the fusion yield per muon [1] [2]. Conventionally muon catalysis is thought to take place in a deuterium-tritium mixture at thermal equilibrium with a well defined global temperature T_g . The fusion cycle rate depends sensitively on temperature through resonant muonic molecule formation. An energetic muon acts, however, like a hot needle plunged into the mixture and the effect is further enhanced because the "needle" is hottest at the tip so that the energy deposition is most effective precisely at the point where the muon is stopped and thus begins the muon-catalyzed fusion cycle. Dissipated kinetic energy from the stopping muon as well as muon binding energy carried by Auger electrons are important heat sources.

The key process of muonic molecule formation takes place at an enhanced effective temperature that depends on the details of energy deposition, thermalization and cooling at the end point of the muon track. A density dependence of the effective temperature and hence the rate of molecular formation is a natural consequence of the thermal spike effect. The observed nonlinear density dependence of molecular formation rates is in agreement with our theoretical estimate.

It is the local temperature at the time τ when the muon reaches the ground state of a muonic tritium atom (μt) that determines the initial μt velocity distribution and hence influences the the rate of muonic molecule formation. To estimate this temperature we note that the average local temperature T_ℓ within a sphere of radius R around the end point of the muon track is,

$$(1) \quad T_\ell = [E_{dep} \left(\frac{4}{3} \pi R^3 \frac{n_1 h d}{2} \phi \right)^{-1} + \frac{N_f(T_g)}{2} k T_g] / \left[\frac{N_f(T_\ell) k}{2} \right]$$

where E_{dep} is the energy deposited within the radius R by the stopped muon, $n_{\text{lh}} = 4.25 \times 10^{22} \text{ atoms cm}^{-3}$ is the liquid hydrogen density, Φ is the relative density in units of n_{lh} and $N_f(T)$ is the effective number of degrees of freedom for diatomic molecules at temperature T . We assume that $N_f(T_{\text{h}}) = N_f(T_{\text{g}}) = 5$, which for the available data set is quite accurate. We shall in the following estimate R and E_{dep} within the time, density and temperature range that is relevant for muon catalyzed fusion.

To calculate R we can almost directly apply methods that have been developed and successfully used [3] [4] to describe the physics of the bubble chamber. The intense energy deposition at the end point of the muon track is, as we shall see, caused by particles - the muon and Auger electrons - that move almost diffusively. A track of practical length $< R$ consists of a significantly longer physical track that is curled up within a sphere of radius R . The radius of a bubble containing the thermal spike at the time τ when a ground state muonic atom just has been formed is given by,

$$(2) \quad R = (4\tau(\Phi)D)^{1/2}.$$

The heat diffusion coefficient $D = D_0/\Phi$ is inversely proportional to density while the cascade time $\tau(\Phi)$ is a more complicated function of Φ . It is unlikely that the bulk heat diffusion coefficient can accurately describe the cooling process at the microscopic length and time scale and the large temperature gradients that are relevant for our purpose. The value of the effective heat diffusion coefficient has been determined from experimental data on bubble formation in hydrogen bubble chambers using a theoretical framework and experimental conditions which are very similar to our case. It was found [4] that $D_0 = 1.23 \times 10^{-3} \text{ cm}^2 \text{ s}^{-1}$ at liquid hydrogen density.

The bulk heat diffusion coefficient at cryogenic temperatures is of the same order of magnitude.

We now calculate the cascade time $\tau(\Phi)$ as a function of density Φ . The density dependence of $\tau(\Phi)$ is due to the competition between external Auger transitions and radiative transitions. Auger transitions are proportional to Φ since this process is driven by molecular collisions. The rates for radiative transitions are independent of density. For $\Phi > .1$ it is sufficient to consider the details of the process starting from $n = 3$. The cascade from higher levels down to $n = 3$ goes almost entirely by Auger transitions or other collisional processes and the total rate $\lambda_{\infty 3}^e$ for this part can therefore be assumed to be proportional to Φ .

The level scheme and the relevant rates are displayed in Fig. 1. We have used decay rates as calculated by Markushin [5] for μd excited atoms. The total deexcitation time can be expressed in terms of these rates as,

$$(3) \quad \tau = \frac{1}{\lambda_{\infty 3}^e} + \left[\lambda_{31}^Y + \left(\frac{1}{\lambda_{32}^Y + \lambda_{32}^e} + \frac{1}{\lambda_{21}^Y + \lambda_{21}^e} \right)^{-1} \right]^{-1}$$

The resulting $\tau(\Phi)$ is shown as a function of density in Fig. 2. and can be inserted in (2) to find the radius of the heated bubble surrounding the initial ground state muonic atom. At $\Phi = 1$ we find that $\tau = \tau_1 = 1.23 \times 10^{-11}$ s leading to a typical size of $R = R_1 = 2.46 \times 10^{-7}$ cm for the thermal spike. The heated region contains 2650 atoms.

We now estimate the energy deposited within this volume. The main sources are the kinetic energy of the muon itself and binding energy released early in the deexcitation cascade. The stopping power for $T_{\mu} = 20 - 500$ eV muons in hydrogen is about $1.6 \times 10^5 \Phi$ keV/cm [6]. Only 40 eV will therefore be deposited along a straight track of length $R_1 = 2.46 \times 10^{-7}$ cm.

The practical penetration depth of slow particles is, however, not equal to the range along the path but is related to the projected range - the penetration depth along the initial direction of the projectile - which because of multiple large angle scatterings can be much shorter than the range along the path. In the standard LSS approach [7] [8] which is based on the assumptions that electronic stopping is dominant and that the projectile is much lighter than the target atoms, the ratio between the projected range r_p and the range along the path r_0 is given by

$$(4) \quad r_p/r_0 = 1 - x \exp(x) \text{Ei}(x), \quad x = MS_n/m_\mu S_e$$

where M is the mass of the target atom and S_n/S_e is the ratio between the "nuclear" stopping power S_n which is due to large momentum transfer processes and the "electronic" stopping power S_e . Assuming an atomic tritium target and inserting $S_n/S_e = .1$ for $T_\mu = 200$ eV as estimated by Wightman [9] we obtain $r_p/r_0 = .2$. With a five times more intense energy deposition close to the end point of the track we estimate the muon kinetic energy deposited within R to be $E_\mu = 5 \times 40$ eV = 200 eV. This result has obviously the character of an order of magnitude estimate. An accurate description of energy deposition on the present length scale would require a Monte Carlo treatment based on a detailed knowledge of the relevant cross sections.

A further contribution to the thermal spike is the binding energy released when the muon falls towards the atomic ground state. From $n \approx 10$ and downwards this energy is carried by Auger electrons or possibly for the last few steps by photons. The practical range R_e of electrons with kinetic energy E is given by the empirical relation [3]

$$(5) \quad R_e(\text{cm}) = c_e E^2(\text{keV})/\Phi, \quad c_e = 8.3 \times 10^{-6} \text{ keV}^{-2} \text{cm}.$$

Comparing with (2) we find that the maximum energy E_{\max} deposited within the heated region is,

$$(6) \quad E_{\max} = (4D_0\Phi\tau/c^2_e)^{1/4}$$

Electrons with energy $E_e > E_{\max}$ will deposit a reduced amount of energy $E_{\text{red}} = E_e - (E_e^2 - E_{\max}^2)^{1/2}$ within a radius $R = (4D_0\tau(\Phi)/\Phi)^{1/2}$. The results in Fig. 2 can be used to obtain $\Phi\tau$ which is found to increase with Φ . At $\Phi = .1$ we find $\Phi\tau = 4.1 \times 10^{-12}$ s so that $E_{\max} = 131$ eV. The corresponding values for $\Phi = 3$ are $\Phi\tau = 2.3 \times 10^{-11}$ s and $E_{\max} = 201$ eV.

Auger transitions dominate the early part of the cascade and are most probable for a minimal change in the principal quantum number n . The binding energy will hence be released as kinetic energy of Auger electrons which is $E_n = 2.69 \text{ keV} \times [n^{-2} - (n+1)^{-2}]$ for the $n+1 \rightarrow n$ transition of muonic tritium. In particular we find that $E_3 = 131$ eV, $E_2 = 374$ eV and $E_1 = 2021$ eV. The $n = 4 \rightarrow 3$ Auger electron is hence always confined within the heated bubble while the maximum contribution from the $n = 3 \rightarrow 2$ and $n = 2 \rightarrow 1$ transitions is 59 eV and 10 eV respectively. The two latter transitions are also often radiative in which case no energy is deposited within the thermal spike. We further note that the $n = 3$ orbital is reached within 10^{-12} s at $\Phi = 1$ while the remaining part of the cascade takes 10^{-11} s. The $n = 3$ level is therefore a natural division point in our model. We shall count the energy released up to this point $E_e = 2.69/3^2 \text{ keV} = 300$ eV as deposited within the heated region. Adding contributions from kinetic and binding energy we find $E_{\text{dep}} = E_\mu + E_e = 200 \text{ eV} + 300 \text{ eV} = 500 \text{ eV}$ which now can be inserted in (1).

To estimate the average temperature within the thermal spike we insert (2) in (1) finding,

$$(8) \quad T_{\ell} = T_1(\tau_1/\tau(\Phi))^{3/2}\Phi^{1/2} + T_g,$$

where $T_1 = T_{\ell}(\Phi=1) = 1750$ K and $\tau_1 = \tau(\Phi=1) = 1.23 \times 10^{-11}$ s. The resulting T_{ℓ} is presented in Fig. 2 as a function of density. It is interesting to note that T_{ℓ} is almost linear in Φ for $\Phi > .3$ and can be written

$$(9) \quad T_{\ell} = -\alpha + \beta\Phi + T_g, \quad \alpha = 430\text{K}, \quad \beta = 2180\text{K},$$

The cycle rate of muon-catalyzed fusion is to a large extent determined by the initial velocity of the ground state muonic atom. We shall in the following argue that this velocity has a thermal distribution with a temperature equal to T_{ℓ} as given by (8) and (9). A 3 keV muon is stopped and captured within less than $10^{-12} \Phi^{-1}$ s [9]. At the moment of capture the muon is by definition located at the centre of the heated bubble. The hot region will now expand with a speed given by (2) or from a microscopic point of view given by the size of the molecular elastic cross section. The time between successive molecular collisions is roughly $10^{-12} \Phi^{-1}$ s which at least for $\Phi > .1$ is much less than the deexcitation time τ (see Fig. 2.). The picture of a muonic deexcitation cascade taking place in a locally thermalized medium appears therefore to be well founded.

Naively one would believe that muonic atoms are "smaller" than normal electronic atoms and hence should diffuse more rapidly than the heat wave so that the thermal spike is quickly left behind. A detailed study of elastic and charge exchange cross sections of excited muonic atoms have been performed by Menshikov and Ponomarev [10]. They found that such cross sections are surprisingly large usually of the order 10^{-16} cm² and hence of the same size as normal atomic and molecular cross sections. Their results indicate that even $n = 2$ muonic atoms are thermalized on a time scale of

$10^{-12} \phi^{-1} \text{ s}$. We can hence conclude that excited muonic atoms will diffuse with roughly the same speed as the heat and that the ground state muonic atom eventually will appear with the same temperature T_g as the surrounding heated medium.

The μt ground state atom can form a muonic molecule either directly or after suffering kinetic energy loss by elastic collisions. The importance of the thermal spike effect is hence decided by the competition between molecule formation and moderation. Molecular formation rates as large as $\lambda_{\text{dt}\mu\text{-d}}(T_g=800\text{K}) = 1.1 \times 10^9 \text{ s}^{-1}$ which corresponds to a cross section $\sigma_{\text{dt}\mu\text{-d}} = 7.5 \times 10^{-20} \text{ cm}^2$ have been reported [1]. Directly measured or reliably calculated elastic cross sections for μt atoms scattering on D_2 , T_2 or DT molecules are not available. The corresponding cross sections for atomic deuterium and tritium have recently been calculated by Melezhik and Ponomarev [11]. For a μt kinetic energy of .15 eV they found for example that $\sigma_{\text{t}\mu\text{+t}} = 1 \times 10^{-20} \text{ cm}^2$ and $\sigma_{\text{t}\mu\text{+d}} = 19 \times 10^{-20} \text{ cm}^2$. Since the Melezhik-Ponomarev calculation obviously is very sensitive to the details of the target structure and the relevant kinetic μt energies is well below the dissociation threshold of hydrogen molecules, cross sections for molecular deuterium and tritium could be very different from the atomic case. We conclude hence that the relation between $\text{dt}\mu\text{-d}$ molecule formation and elastic scattering cross sections are essentially unknown but that they probably are of the same order of magnitude.

The rapidly decaying transient in the observed [12] cycle rate at $\phi = 0.01$ has been taken as an indirect confirmation of the view that moderation is much faster than molecule formation. Assuming high initial velocities of muonic atoms the observed transient were explained [13] [14] as a reflection of the finite thermalization time combined with velocity dependent molecular formation rates.

Theoretical uncertainties hamper however any firm conclusion. The initial nonequilibrium velocity distribution of μt atoms is essentially unknown at such low densities where the lack of complete local thermalization makes the final velocity sensitive to recoil effects during the deexcitation cascade. The moderation of μt atoms was calculated using cross sections for atomic deuterium and tritium which according to the preceding discussion is a rather crude approximation. Since the effect of molecule formation on the time evolution of the μt velocity distribution was not taken into account in Ref. 13 it is not clear from their results that moderation always must be much faster than molecule formation.

We shall here avoid any detailed assumption concerning the relation between moderation and molecule formation rates and focus on qualitative predictions of the thermal spike model. We note that the effect of moderation will be to reduce the excess temperature T_1 in (8) and thus keeping the ratio $\alpha/\beta = .20$ in (9) constant. The reduction in the excess temperature will, however, be independent of density since the both elastic and molecule formation rates are proportional to Φ . We shall in the following suggest methods by which the size of the thermal spike effect can be extracted from data.

To study the effects of thermal spikes in muon catalyzed fusion we shall focus on the rate $\lambda_{\text{dt}\mu\text{-d}}$ of muonic molecule formation: $\mu\text{t} + \text{D}_2 \rightarrow \mu\text{td-d}$ where the μdt molecule briefly acts as a positive centre in a hydrogenlike electronic molecule. Since this process includes a resonant mechanism - the binding energy of the muonic molecule must be absorbed within the host molecule - it is a sensitive probe of the initial relative velocity of the μt atom and the D_2 molecule.

Because of the small elastic cross section ($10^{-20} - 10^{-19} \text{ cm}^2$) and long molecular formation time (10^{-9} s) the ground state muonic atom will leave the heated region and form a muonic molecule in the colder ($T = T_g$) sur-

rounding medium. Adding the different velocity distributions of μt atoms and D_2 or DT molecules we obtain, since $\lambda_{dt\mu-d}$ depends only on the relative velocity, the effective temperature of molecular formation,

$$(10) \quad T_{\text{eff}} = [(m_d + m_x)T_\ell + m_{\mu t}T_g]/(m_d + m_x + m_{\mu t})$$

where m_x equals m_d or m_t depending on the composition of the host molecule.

The initial ground state muonic atom can be a $(\mu t)_{1S}$ or a $(\mu d)_{1S}$ atom. The probability for the latter case is usually written $q_{1S}C_d$ where C_d is the relative deuterium concentration and q_{1S} is a correction that takes into account that muons bind harder to tritons than to deuterons throughout the deexcitation process.

A muon in a $(\mu d)_{1S}$ atom will within 10^{-9} s transfer to a triton by the exotherm reaction $(\mu d)_{1S} + t \rightarrow (\mu t)_{1S} + d$. Since the energy released in the transfer reaction is two orders of magnitude larger than the initial kinetic energy we shall assume that the rate for molecular formation after a transfer reaction $\lambda_{dt\mu-x}^t$ is independent of T_g and T_ℓ . Ignoring any possible effect of triple collisions we shall here make the simplest possible assumption for the density and temperature dependence of molecular formation rates.

$$(11) \quad \lambda'_{dt\mu-d} = q_{1S}C_d\lambda_{dt\mu-d}^t + (1 - q_{1S}C_d)\lambda_{dt\mu-d}(T_{\text{eff}})$$

where $\lambda'_{dt\mu-d}$ is the observed normalized molecular formation rate that depends of global temperature and density and $\lambda_{dt\mu-d}$ is the normalized physical molecular formation rate in the direct channel depending only of the effective temperature ((normalized rate) = (measured rate)/ Φ). Combining (9) and (10) we get,

$$(12) \quad T_{\text{eff}} = a(-\alpha + \beta\Phi) + T_g, \quad a = 2m_d/(2m_d + m_{\mu t}) = .56$$

Measured molecular formation rates depend nonlinearly on density [1]. This effect is not completely understood but it is usually thought [15] to be due to some three-body effect where energy is carried away by a third object so that the μt -D₂ resonance can be better tuned. It is, however, obvious that nonlinear density dependence would be generated by the thermal spike effect. This prediction can be tested experimentally without any assumptions concerning $\lambda'_{dt\mu-d}(T_{\text{eff}})$. Taking derivatives of (11) with respect to Φ and T_g we find that the slopes of the temperature and density distributions of $\lambda'_{dt\mu-d}$ at the same point in the (T_g, Φ) plane is related by,

$$(13) \quad \frac{\partial \lambda'_{dt\mu-d}}{\partial \Phi} = a\beta \frac{\partial \lambda'_{dt\mu-d}}{\partial T_g}$$

This relation can be used to measure β . Experimental information on the size of the thermal spike effect would, because of the crude nature of the theoretical estimates, be very useful. To improve the statistical significance one should plot experimental results as a function of $T_{\text{eff}} = -a(\alpha + \beta\Phi) + T_g$. We predict that $dt\mu-d$ molecular formation rates are equal along this line in the (T_g, Φ) plane. By this procedure other effects could be probed more efficiently.

Measured density and temperature distributions of $\lambda'_{dt\mu-d}$ are often produced by integrating over some temperature or density range. Since (11) refers to a given point in a (Φ, T_g) plane it is difficult to compare the model with integrated distributions. The model predictions should instead be tested directly against a complete data set.

We can, however, use the results in Ref. 1 where data for $\lambda'_{dt\mu-d}$ were fitted to the form,

$$(14) \quad \lambda'_{dt\mu-d} = \lambda^{(1)}_{dt\mu-d} + \Phi \lambda^{(2)}_{dt\mu-d},$$

and the temperature dependent parameters were given for three different temperature intervals (see the table). To get a linear Φ dependence in our model we must assume that $\lambda_{dt\mu-d}(T_{eff})$ is a linear function of T_{eff} . We note that $\lambda_{dt\mu-d}(T_{eff})$ as calculated in the "direct formation model" [13] within the range $T_{eff} = 100 \text{ K} - 1250 \text{ K}$, is well described by

$$(15) \quad \lambda_{dt\mu-d}(T_{eff}) = C_1 + C_2 T_{eff}.$$

Comparing with the T_g and Φ range employed in Ref. 1 it appears that the experimentally probed T_{eff} falls well within the required range for the linear approximation (15) to be valid.

Combining (11), (12) and (15) we obtain a simple expression for the measured molecular formation rate,

$$(16) \quad \lambda'_{dt\mu-d} = \kappa_1 + \kappa_2 T_g + \kappa_3 \Phi,$$

$$\kappa_1 = q_{1S} C_d \lambda^{(1)}_{dt\mu-d} + (1 - q_{1S} C_d) (C_1 - C_2 a \alpha),$$

$$\kappa_2 = (1 - q_{1S} C_d) C_2 T_g,$$

$$\kappa_3 = a \beta \kappa_2$$

where $a = 2m_d / (2m_d + m_{\mu t}) = .56$, $\alpha = 430 \text{ K}$ and $\beta = 2180 \text{ K}$. The relation $\kappa_3 = a \beta \kappa_2$ between the temperature and density slopes is according to (13) a generic feature in our model. Since (14) and (16) have the same form we can directly compare the parameters. We first use the experimental information on the temperature dependence finding $\kappa_1 = 216 \times 10^6 \text{ s}^{-1}$ and $\kappa_2 =$

$0.3 \times 10^6 \text{ s}^{-1} \text{K}^{-1}$. The result of this linear fit to $\lambda^{(1)}_{dt\mu-d}$ is displayed in the table and is in fair agreement with data.

All parameters in (16) are now defined and we can use the model, now including experimental information on the temperature dependence, to predict the density dependence. It is obvious that (16) permits no temperature variation in $\lambda^{(2)}_{dt\mu-d}$. Finding $\lambda^{(2)}_{dt\mu-d} = \kappa_3 = 367 \times 10^6 \text{ s}^{-1}$ for all temperatures we have an agreement with measured values of $\lambda^{(2)}_{dt\mu-d}$ within at worst 1.7 standard deviations (see the table). Considering the crude approximations made along the way this is a surprisingly good result. If our estimate of the local temperature is correct this implies that molecule formation is faster than moderation within the considered temperature and density range.

The observed [1] rate $\lambda_{dt\mu-t}$ for $dt\mu$ formation within a DT host molecule is an order of magnitude smaller than the dominant rate $\lambda_{dt\mu-d}$. The rate of elastic scattering is then, according to the discussion above, probably significantly larger than $\lambda_{dt\mu-t}$. It is therefore reasonable to assume that μt atoms either have formed a $dt\mu$ molecule via the fast $dt\mu-d$ channel or have been moderated to a velocity corresponding to the global temperature T_g before they enter the slow $dt\mu-t$ channel. We therefore expect $\lambda_{dt\mu-t}$ to be independent of density. This simple argument is in good agreement with measurements since no significant density dependence of $\lambda_{dt\mu-t}$ was seen [1].

The calculated [13] $dt\mu-d$ formation rate goes through a broad maximum at $T_{\text{eff}} = 1700 \text{ K}$ and then falls slowly with increasing T_{eff} . The thermal spike model suggests that optimal $\lambda_{dt\mu-d}$ can be reached by increasing density at cryogenic temperature. We get the theoretical optimum $T_{\text{eff}} = aT_\ell = 1700 \text{ K}$ at density $\Phi = 1.6$.

The new generation of μCF -experiments at LAMPF [1] will achieve densities of $\Phi = 2.3 - 2.7$ at cryogenic temperatures which in our model means

$T_{\text{eff}} = 2570 - 3060$ K. This is well above any predicted optimum temperature for molecular formation. We hence predict that $\lambda_{\text{dt}\mu\text{-d}}$ will be seen to saturate with respect to both Φ and T_g in the new LAMPF experiment.

References

- [1] S.E. Jones et al., *Phys. Rev. Lett.*, 56 (1986) 588.; S.E. Jones, Proc of Workshop on Muon Catalyzed Fusion and Fusion with Polarized Nuclei, Erice, April 3-9 1987.
- [2] For a recent review see C. Petitjean et al, SIN preprint PR-87-07 and Proc. of Int. Symp. on Muon Catalyzed Fusion, Leningrad, May 26-29 1987.
- [3] F. Seitz, *The Physics of Fluids*, 1 (1958) 2.
- [4] Yu. A. Aleksandrov et al, "Bubble Chambers", Indiana Univ. Press Bloomington 1967.
- [5] V.E. Markushin, *Zh. Eksp. Teor. Fiz.* 80 (1981) 35 (*Sov. Phys. JETP* 53 (1981) 16).
- [6] J.S. Cohen, *Phys. Rev. A*, 27 (1983) 167.
- [7] H.E. Schiott, *Mat. Fys. Medd. Dan. Vid. Selsk.*, 35 no. 9 (1966).
- [8] J.F. Ziegler, *The Stopping and Ranges of Ions in Matter*, Vol 3, Pergamon Press.
- [9] A.S. Wightman, *Phys. Rev* 77 (1950) 521.
- [10] L.I. Menshikov and L.I. Ponomarev, *Z. Phys. D*, 2 (1986) 1.
- [11] V.S. Melezhik and L.I. Ponomarev, *Zh. Eksp. Teor. Fiz.*, 85 (1983) 434 (*Sov. Phys. JETP* 58 (1983) 254).
- [12] W.H. Breunlich et al., *Phys. Rev. Lett.* 53 (1984) 1137.
- [13] J.S. Cohen and M. Leon, *Phys. Rev. Lett.*, 55 (1985) 52.
- [14] P. Kammel, *Lettere al Nuovo Cimento* 43 (1985) 349.
- [15] L.I. Menshikov and L.I. Ponomarev, *Phys. Lett.* 167B (1986) 141.

FIGURE CAPTIONS

- FIG. 1. Deexcitation scheme for μd transitions of importance for the density dependence of the deexcitation time. Values of rates are taken from Markushin (Ref 5) and expressed in units of 10^{12} s^{-1} . λ_{ij}^{Y} and λ_{ij}^{e} are radiative and Auger rates respectively for the $i \rightarrow j$ transition.
- FIG. 2. The local temperature T_{L} (solid line) at the time τ when the μt or μd atom reaches the ground state is shown together with τ (dashed line). The global background temperature T_{g} is assumed to be zero.

Table 1:

Calculated temperature and density dependence of $\lambda_{dt\mu-d}$ is compared with data [1] assuming:

$$\lambda_{dt\mu-d} = \lambda_{dt\mu-d}^{(1)} + \lambda_{dt\mu-d}^{(2)}\Phi \text{ (units in } 10^6 \text{ s}^{-1}\text{)}.$$

Theoretical "errors" reflects the size of experimental temperature bins.

T_g (K)	$\lambda_{dt\mu-d}^{(1)}$ (data)	$\lambda_{dt\mu-d}^{(1)}$ (theory)	$\lambda_{dt\mu-d}^{(2)}$ (data)	$\lambda_{dt\mu-d}^{(2)}$ (theory)
< 130	206±29	235±19	450±50	367
300	306±43	306	286±67	367
400-500	347±52	351±15	275±120	367

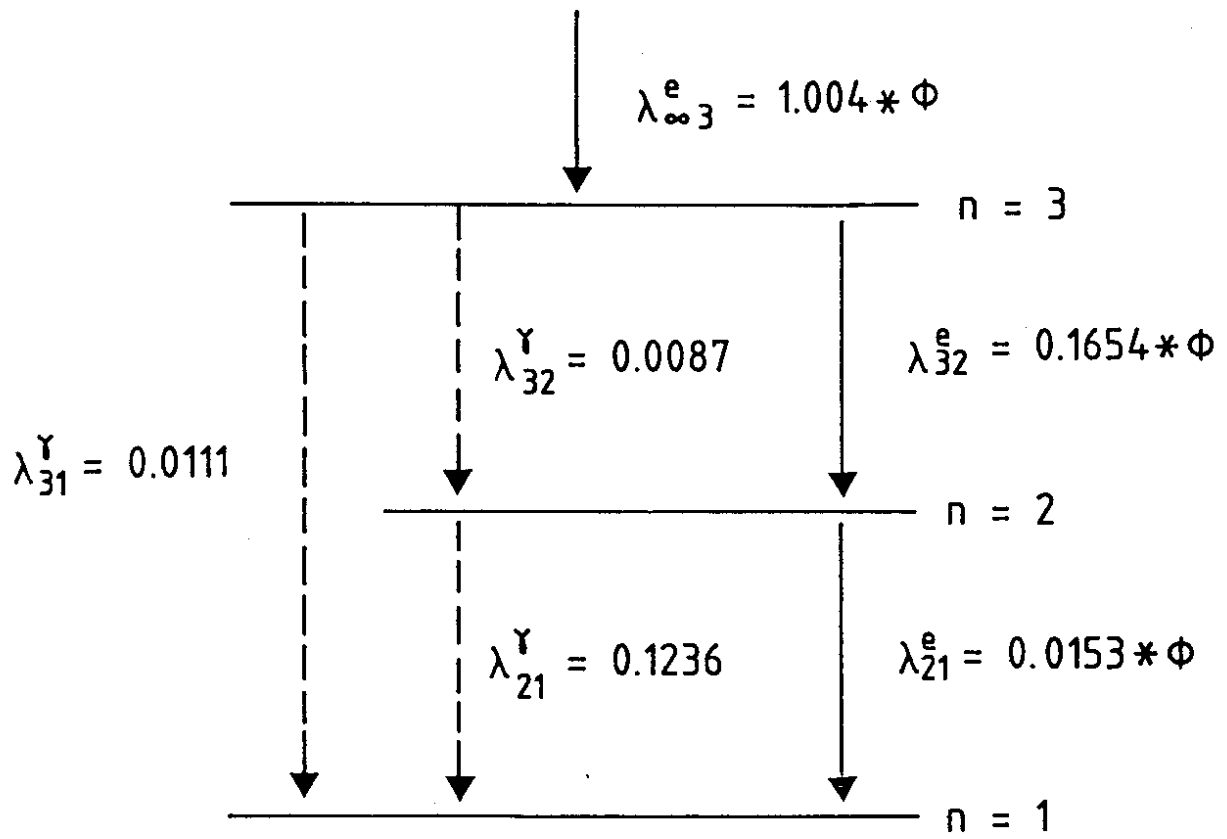


FIG. 1.

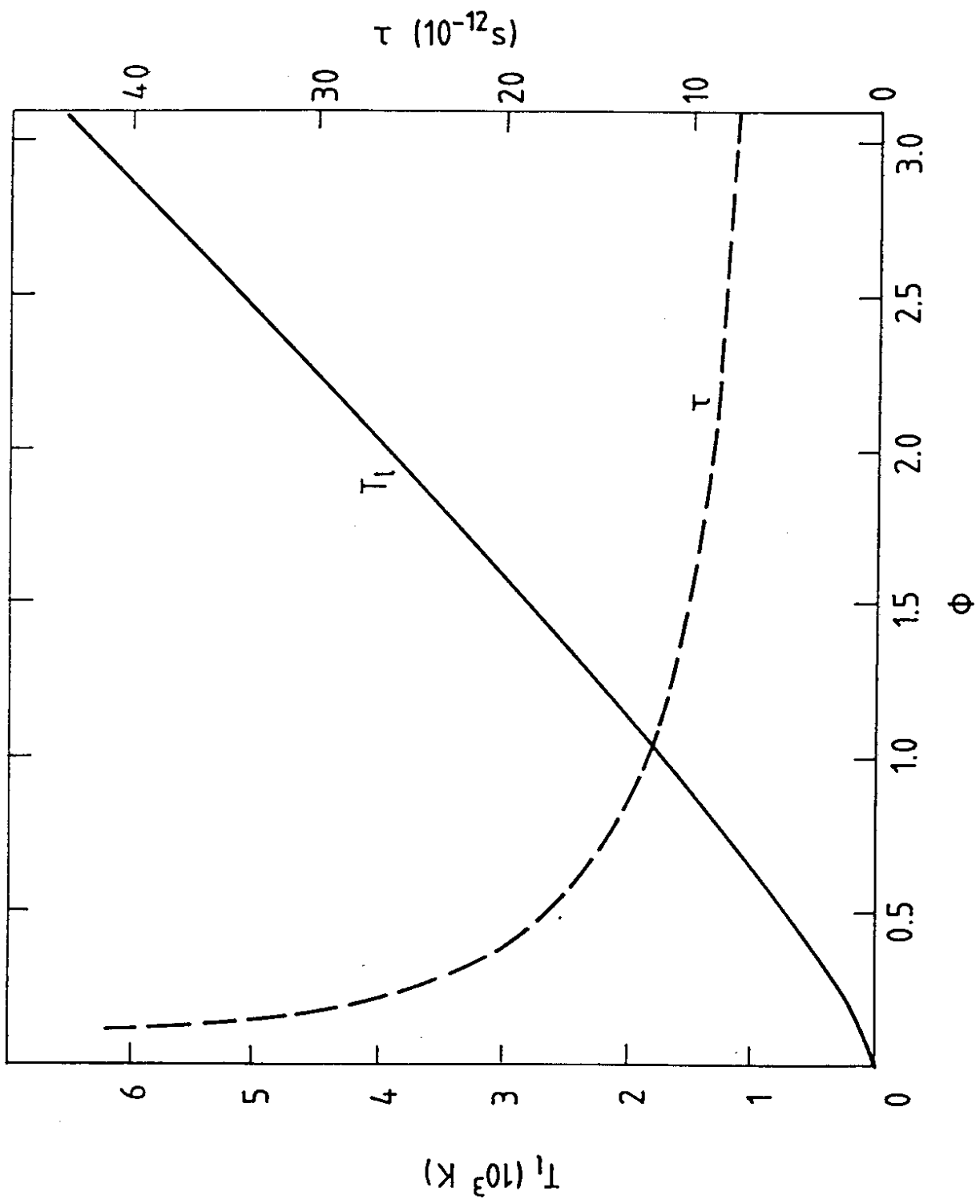


FIG. 2.